Numerical analysis of the impact of rotor and screen hole plate design on the performance of a vertical pulper

MARCUS BRITZ, BETTINA GRASHOF, AXEL GOMMEL, GERT GOTTSCHALK, OLIVER LUEDTKE, AND WOLFGANG MUELLER

ABSTRACT: The dissolving of mechanical pulp is one of the most important process steps in stock preparation, since pulping occurs at the very beginning of the papermaking process. Efficient mixing of the pulp in a short amount of time is essential to achieve high furnish volume flow rates. The design of the rotor, as well as the pulper vat and inserts, significantly affects the overall performance of the pulper, such as mixing efficiency and power demand. Using advanced numerical methods such as computational fluid dynamics (CFD) can accelerate the development process. The CFD simulations allow for detailed analysis of flow phenomena, making it possible to study a real-size machine numerically. This approach is particularly advantageous because it can reduce the need for time-consuming and costly experiments associated with scaling up test rigs.

In this study, we compared two different rotor designs utilized in a vertical pulper and evaluated the numerical results with experimental data. Rotor A is designed for low turbulence and low power demand, while rotor B is designed for high turbulence with high power demand. The CFD results showed good agreement with the experimental measurements. We investigated how the rotor design influences the free fluid surface and the mixing efficiency. Our study also highlights the differences in results depending on whether water or furnish is simulated, which exhibit Newtonian or, respectively, non-Newtonian fluid behavior.

Additionally, a detailed numerical investigation of various screen hole plate designs revealed that the newly developed hole design significantly reduces pressure loss compared to a standard drilled hole. This outcome was consistent for both types of fluids investigated: water and furnish.

Application: A CFD simulation is a state-of-the-art, powerful numerical tool to get a better understanding of the complex flow phenomena that occur within the pulp mixing process. Furthermore, the development of new pulper products is faster and more cost-efficient.

The pulping process relies on the well-established principle of mixing that is familiar within the field of process engineering. The primary objective is to create a fiber suspension by combining fibers and water. Both mixing efficiency and power consumption are critical quality criteria in the pulping process. For example, the design of the casing (such as baffles) and the rotor can significantly affect the overall mixing efficiency. Additionally, the position of the rotor (centric or eccentric) also influences the level of turbulence generated [1].

The general design concept of a pulper is illustrated in **Fig. 1**, using Voith's IntensaPulper as an example. The pulper is filled either discontinuously or continuously with fibers and water. The kinetic energy of the rotor is con-

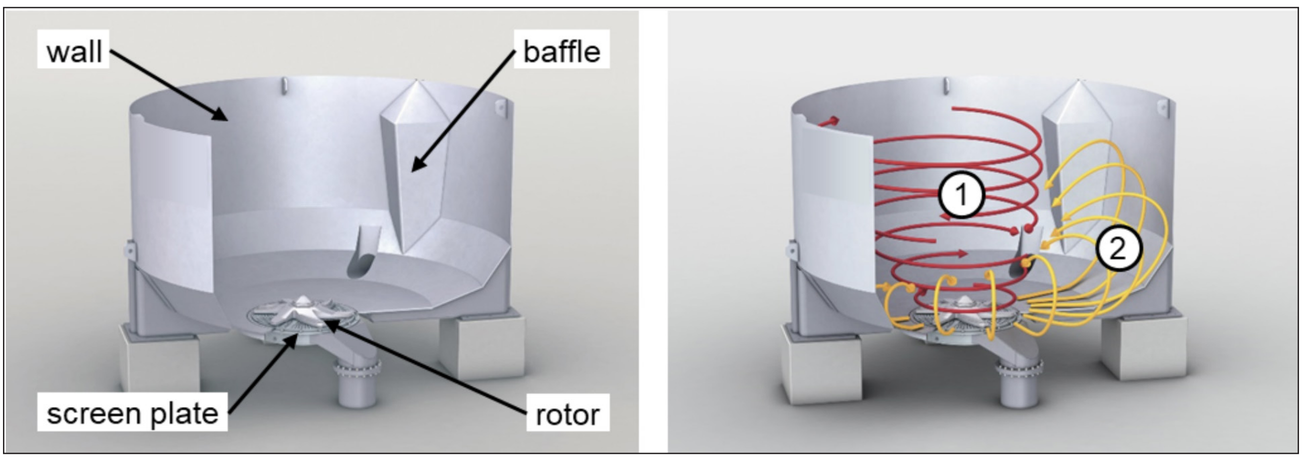

1. General design configuration of a pulper (left) and its main vortices (right) [2].

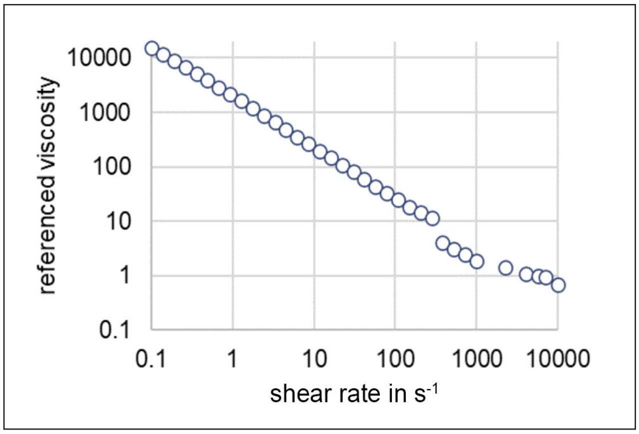

2. Rheological measurement data used to define furnish for flow simulation [12].

verted into fluidic energy, causing the fluid within the pulper to move and form two main vortices: (1) a vortex that follows the rotor's motion, with swirl formation visible at the free surface; and (2) the flow hits the pulper wall, rolls up, and feeds fluid back into the main swirl. A screen plate (or extraction plate) is installed between rotor and outlet tube to separate coarse contaminants. The rotor, in combination with bars on the screen plate, helps to reduce the formation of flakes.

Nowadays, the pulping process can be effectively modeled using advanced numerical tools like computational fluid dynamics (CFD). However, the CFD simulation of a pulper is challenging due to the free surface created by the fluid inside the pulper and the surrounded air [3]. Consequently, several researchers have concentrated on developing numerical methods and approaches for turbulent mixing, such as those used in stirred-tank reactors [4,5]. Another significant challenge is modeling the furnish due to its non-Newtonian fluid behavior and incorporating this into CFD simulations [6-11].

We defined the non-Newtonian fluid behavior of the used fiber suspension with 4% consistency in our CFD simulations using a rheological model based on experimental data, as shown in **Fig. 2**. The measurement points are fitted and the rheological model of the fiber suspension is mathematically defined as followed:

$$\eta(\dot{\gamma}) = \begin{cases} \eta_{\text{max}} = \eta(\dot{\gamma} = 1\,1/s) & \text{if } \dot{\gamma} \leq 1\,1/s \\ \eta_{\text{max}}\,\dot{\gamma}^{N} & \text{otherwise} \\ \eta_{\text{min}} = \eta_{\text{water}} & \text{if } \eta \leq \eta_{\text{water}} \end{cases} \quad (1)$$

where η stands for the dynamic viscosity, $\dot{\gamma}$ for the shear rate, and N for the dimensionless flow behavior index.

ROTOR DESIGN

The main idea behind generating a numerical model of a pulper is to create a virtual test rig that can support the product development. Within this virtual test rig, various designs can be implemented similarly to how they would be in a real test rig. To achieve this, measurement data from a real test rig are essential for calibrating the numerical model and its methods, such as turbulence modeling. By doing so, multiple designs can be tested and evaluated virtually without the need to manufacture any physical rotors. In our case, we were particularly interested in assessing the power consumption and fluid turbulence trends associated with different rotor design strategies. This method of digital testing is analogous to the approach used in a real test rig, where different rotor designs are replaced, tested, and compared to each other.

Setup of numerical model

The investigated geometry exemplifies a common pulper design. Our numerical model includes both the pulper casing and the rotor, as shown in **Fig. 3**. We performed the CFD simulations using Ansys Fluent software version 2021

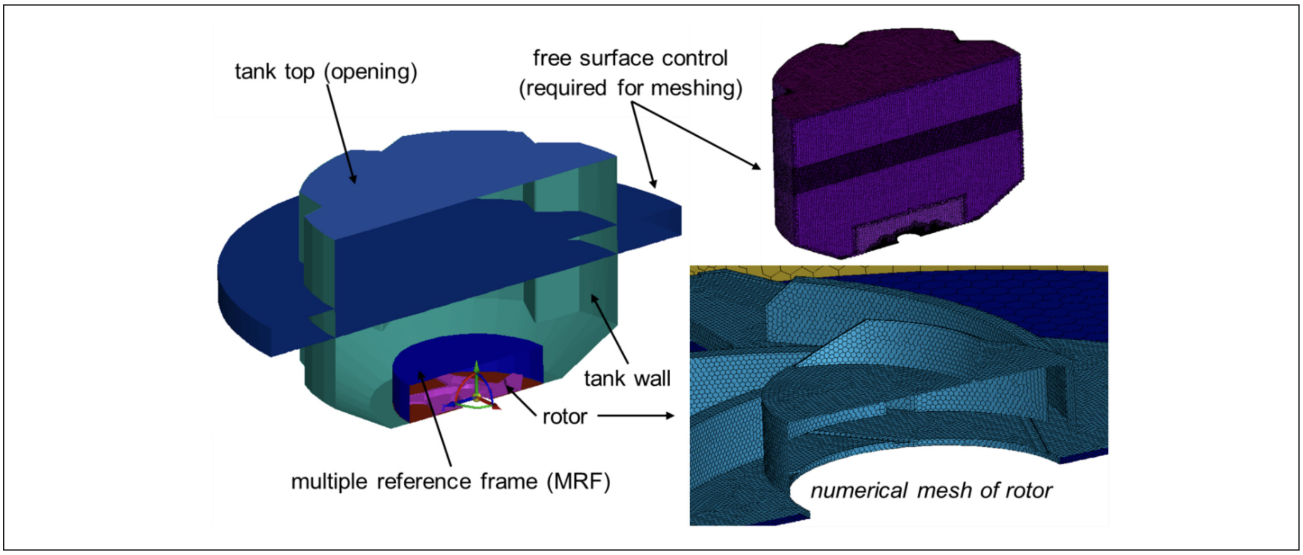

3. General numerical setup (left); mesh (right, top); and detail of rotor mesh (right, bottom).

Fill Level	Ambient Pressure	Fluid Temperature	Rotor Speed
Constant (starting condition)	0 Pa (reference)	40°C	Variable

I. General numerical boundary conditions for pulper's computation fluid dynamics (CFD) simulation.

Rotor Design	Turbulence	Power Demand
Rotor A Rotor B	Low High	Low High

II. General numerical boundary conditions for pulper's CFD simulation.

R2 (Ansys; Canonsburg, PA, USA). We were able to keep the mesh size small, resulting in about 3 million elements, by utilizing Fluent's poly-hexcore meshing technology. The steady and rotating domains were connected via an interface using a frozen rotor or rather a multiple reference frame (MRF) approach [13]. Menter's Shear Stress Transport (SST) turbulence model was used to model the turbulence [14], and the curvature correction modification was applied to accurately model the strong vortex formation. We used the Volume of Fluid method (VOF) to model and resolve the free surface of the pulper [15]. This is particularly important for examining the impact of rotor design on the swirl, which can be easily observed based on the free surface formation. We simulated the pulper as quasi transient, focusing on the averaged operating condition. To simplify the numerical model, the screen plate located below the rotor was omitted and the open space was closed with a wall. All walls were assumed to be adiabatic and hydraulically smooth.

The other numerical boundary conditions can be taken from **Table I**. The virtual pulper is filled with a specified volume, defined by the same fill level across all investigated cases. The only variable parameter was the rotational speed of the rotor.

The two rotors examined in this study are designed based on different mixing strategies and are listed in **Table II**. These selected rotors vary significantly in terms of turbulence and power demand, allowing us to clearly distinguish the differences in their general functional principles.

Validation of numerical model

Generally, it is recommended to validate a numerical model before using it for extensive numerical studies, e.g., design or parameter variation. Therefore, we used measurement data from rotor B to quantitatively assess the accuracy and physical plausibility of the generated numerical model and the methods used for the pulper. **Figure 4** shows the power as a function of the rotational rotor speed of the numerical (NUM) and experimental (EXP) data. All data are referenced to the experimental power value of water at maximum rotor speed. The power was numerically determined based on the torque.

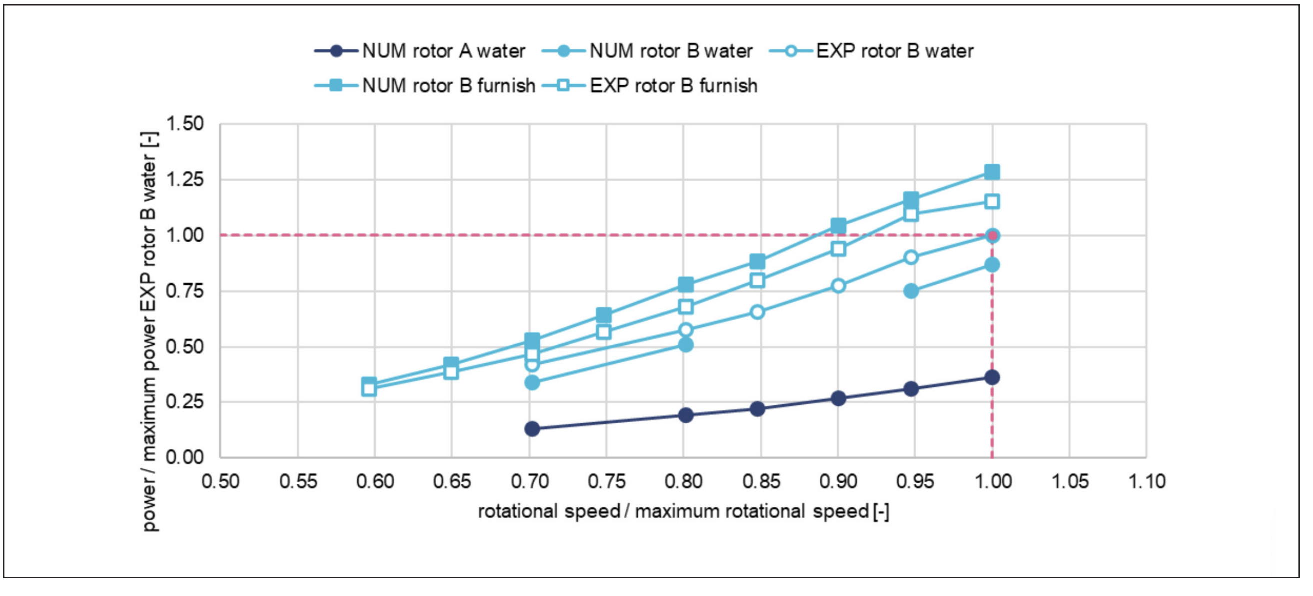

4. Numerical (NUM) and experimental results (EXP) of power consumption.

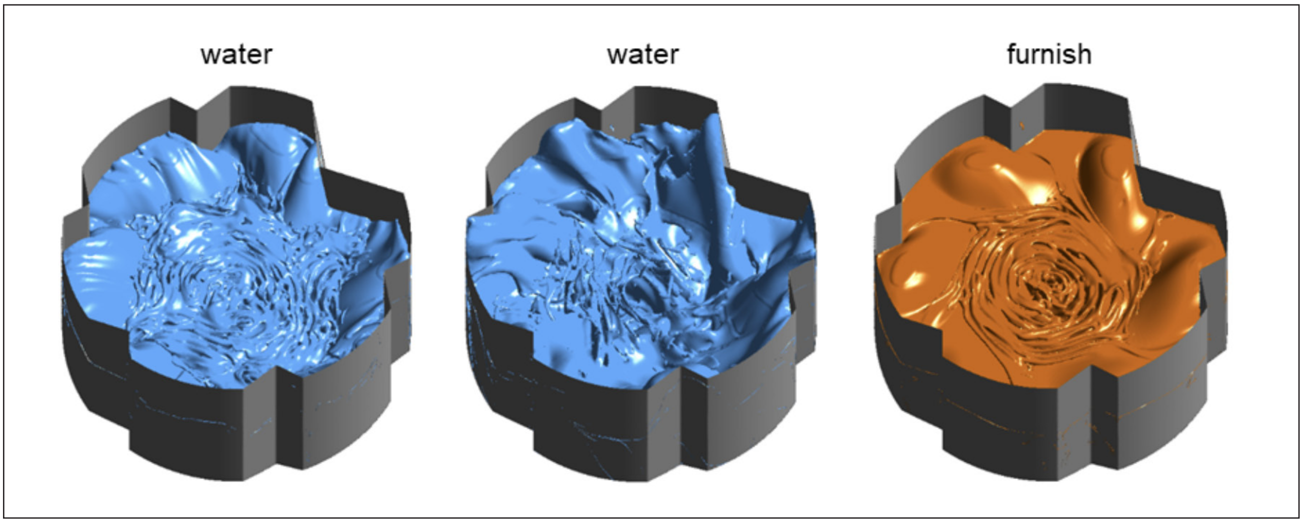

5. Fluid surface of rotor A (left) and rotor B (middle, right) for maximum rotor speed.

We encountered difficulties simulating two operating points of rotor B with water, as the swirl reached the bottom of the tank, causing significant numerical instabilities and resulting in a non-converged solution. Consequently, there is a lack of numerical information for power consumption within this operating interval. However, there is an overall good quantitative agreement between the numerical and experimental results for both water and furnish. The comparison of the data also shows that trends are consistent. For rotor B, the power demand for furnish is higher than for water and the curves for water and furnish diverge with increased rotor speed.

Furthermore, the numerical results reflect the differences in rotor design strategies. In contrast to rotor B, which requires high power consumption to generate high turbulence in the fluid, rotor A is designed for low turbulence, resulting in lower power consumption. This result confirms that designing a rotor is always a compromise between turbulence production, which impacts velocity magnitude and mixing time, and power consumption. Therefore, rotor design is a critical factor in achieving the required mixing quality while considering energy costs.

Detailed flow analysis

As a result of the rotating rotor and the stationary pulper wall, the rotor-dependent fluid surface is formed, which is visualized for water in **Fig. 5**. For both rotors, the two main vortices can be identified: the swirl located above the rotor and the vortex near the wall. The fluid surface formed by rotor B appears significantly more turbulent compared to that of rotor A. This circumstance qualitatively aligns with their respective design strategies. Additionally, the fluid surface confirms the functionality of the baffles. There is an interaction between the rotating fluid volume and the

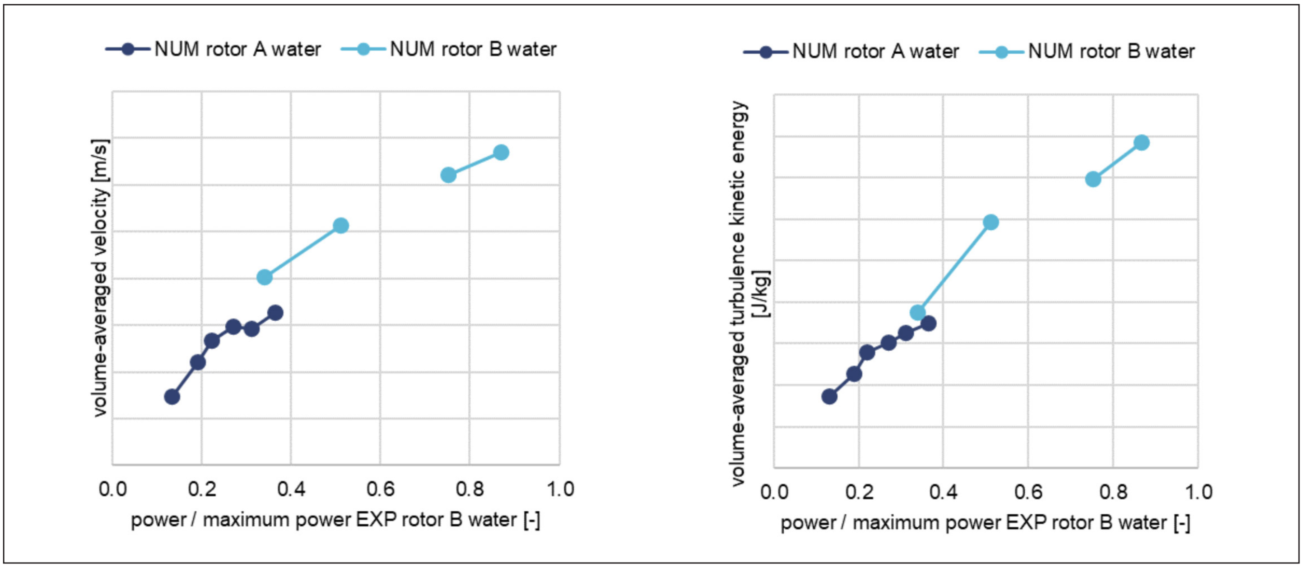

6. Volume averaged velocity (left) and turbulence kinetic energy (right).

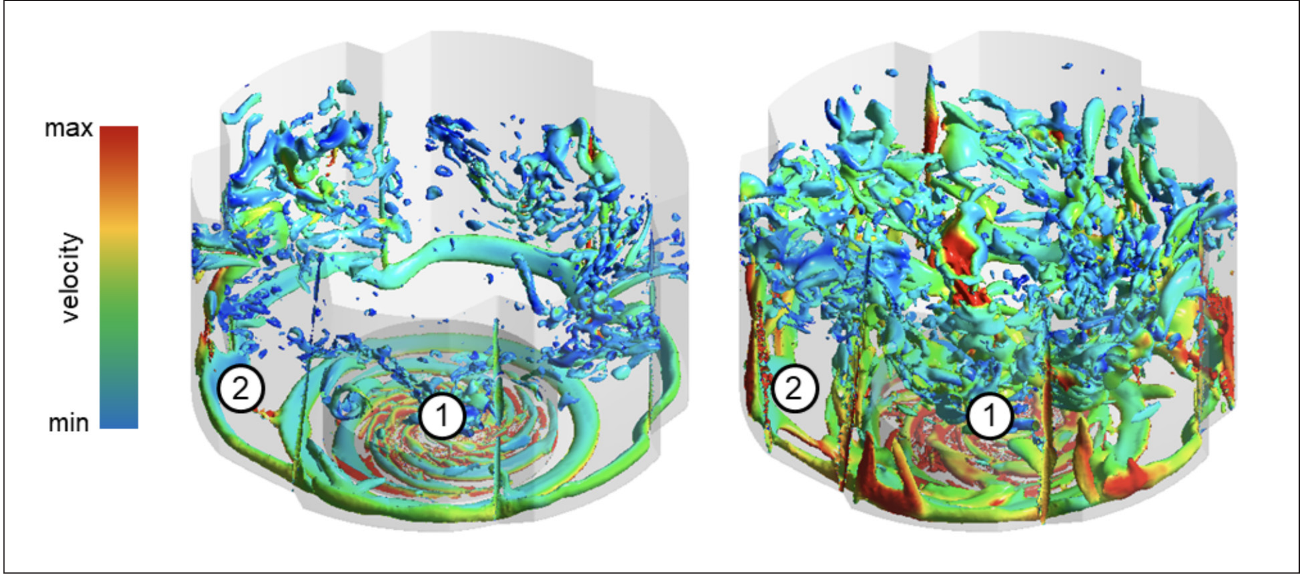

7. Vortex structures of rotor A (left) and rotor B (right), visualized on isosurface with constant Q value, which is a measure of the relative dominance of rotational vs. stretching deformation within a fluid element.

stationary baffles, resulting in wave formation. This interaction leads to localized high turbulence production, thereby improving overall mixing.

Additionally, the impact on fluid behavior is demonstrated in Fig. 5, where the fluid is defined as fiber suspension according to the previously introduced rheological model. As expected, the small shear rates on the fluid surface led to a higher dynamic viscosity, and consequently, higher fluid friction due to the non-Newtonian fluid behavior. This results in reduced local turbulence, which is indicated by the smoother fluid surface.

The movement of the entire fluid volume in the pulper, caused by the rotor, can be used as an indicator of the amount of turbulence. In this context, the volume-averaged velocity and turbulence kinetic energy are shown in **Fig. 6**. An increase in the fluid's velocity directly leads to an increase in turbulent kinetic energy distributed throughout the pulper volume.

A typical way to visualize three-dimensional vortex structures of a turbulent flow field is the Q criterion, which is defined as follows:

$$Q = \frac{1}{2}\left(\left\|\Omega_{ij}\right\|^2 - \left\|S_{ij}\right\|^2\right) = -\frac{1}{2}\frac{\partial U_i}{\partial x_j}\frac{\partial U_j}{\partial x_i} \quad \text{with} \quad \Omega_{ij} = \frac{1}{2}\left(\frac{\partial U_i}{\partial x_j} - \frac{\partial U_j}{\partial x_i}\right) \qquad (2)$$

Here, S_{ij} stands for the shear tensor; Ω_{ij} is the rotation of the flow vector field; and U is the local flow velocity in i,j-direction at local position x. The Froebenius matrix is indicated by $||\ldots||$. The local equilibrium of both quantities (shear rate and rotation) is described by the Q criterion in all three directions in space. By visualizing an isosurface with a constant Q value, the pulper's vortex structure can be investigated in detail, as is shown in **Fig. 7**.

The two main vortices, swirl (1) and the one close to the wall (2), can be clearly seen. Especially in the case of rotor B, a strong vortex formation is evident, indicated by both the larger size and the higher velocity values compared to rotor A. Furthermore, the vortex structures caused by rotor B are finer, which implies higher turbulence. This increased turbulence is beneficial for reducing the mixing time, thus enhancing the mixing efficiency of the entire pulping process.

SCREEN HOLE PLATE DESIGN

The design of the screen plate has major impact on the functionality of the pulper. Specifically, the pressure loss, which depends on the hole design and open surface, significantly influences the rotor function and the hydraulic capacity of a continously working pulper. Therefore, it is worthwhile to investigate the impact of the screen plate design on the resulting pressure loss and flow field in detail. Understanding these effects can lead to optimizations that enhance the overall efficiency and effectiveness of the pulping process.

Setup of the numerical model

The numerical model and setup used in our investigation are shown in **Fig. 8**. We neglected the rotor in our model, because the primary focus was on the general hole design of the screen plate. Simulating the entire screen plate would be computationally too intensive, so we developed a strategy to minimize the computational effort.

The quantity of interest in our numerical investigation was the pressure loss. Since the pressure is a thermody-

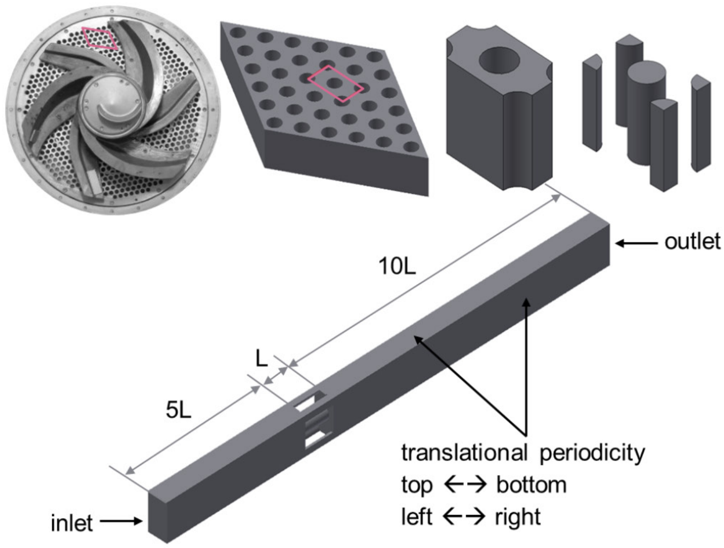

8. Strategy of numerical model generation (top) and numerical setup (bottom) of screen hole plate.

namic intensive state variable, the results from the reduced model can be directly applied to the full screen plate. Consequently, the two-hole geometry used in our numerical model consists of one center hole plus four quarter holes. This configuration considers two main aspects of the screen plate: the hole design itself and the open surface area. This approach allows us to accurately assess the impact of the screen plate design on pressure loss while keeping computational requirements manageable.

Since the fluid hits the screen plate wall, the dynamic pressure is transformed into static pressure. This pressure information is transported upstream due to the subsonic flow field. On the other hand, as the flow is accelerated within the hole, a strong fluid jet with a high velocity is formed. The fast jet mixes with the surrounded slower flow due to friction, a process that requires space defined by the mixing-out length. To ensure that these flow phenomena do not distort the numerical results, we extended the numerical domain by five times the screen plate thickness in the upstream direction and 10 times in the downstream direction.

All numerically investigated hole geometries have the same hole diameter. Design A is a single-hole and represents the simplest geometry type. Design B is chamfered, design C is counter-sunked, and design D combines the features of designs B and C. By examining these various designs, we aim to understand how different hole geometries impact the pressure loss and flow characteristics in the screen plate.

We performed the CFD simulations using Ansys CFX software version 2019 R3. Analogous to the previously shown numerical model of the entire pulper, Menter's SST turbulence model was used to model the turbulence [14]. This approach ensures that the numerical results can be directly transferred between both CFD simulations. All walls were assumed to be adiabatic and hydraulically smooth. The mesh generation of all hole geometries was done by using Ansys ICEM, resulting in an unstructured mesh consisting of about 6 million tetrahedral elements. The boundary layer was resolved with 10 hexahedral cells [16]. The numerical boundary conditions are listed in **Table III**. The rheological model defined by Eq. 1 was used to define the fiber suspension, ensuring consistency in the simulation parameters.

Numerical results

The pressure loss was determined as the static pressure difference between the inlet and outlet. The results for both water and furnish as fluids are shown in **Fig. 9** for all four investigated hole geometries. The pressure loss increases with increased flow velocity. The pressure loss trend for the hole geometries is consistent for both fluid types: A > B > C > D. For water, a Newtonian fluid, the pressure loss is independent of shear rate due to the constant viscosity. The change of pressure loss aligns with basic theory of fluid mechanics, as the pressure loss of incompressible Newto-

Inlet Velocity	Inlet Flow Angle	Outlet Pressure	Fluid Type
Variable	0° (axial flow)	0 Pa (reference)	Water, Furnish

III. Numerical boundary conditions of hole geometry CFD simulations.

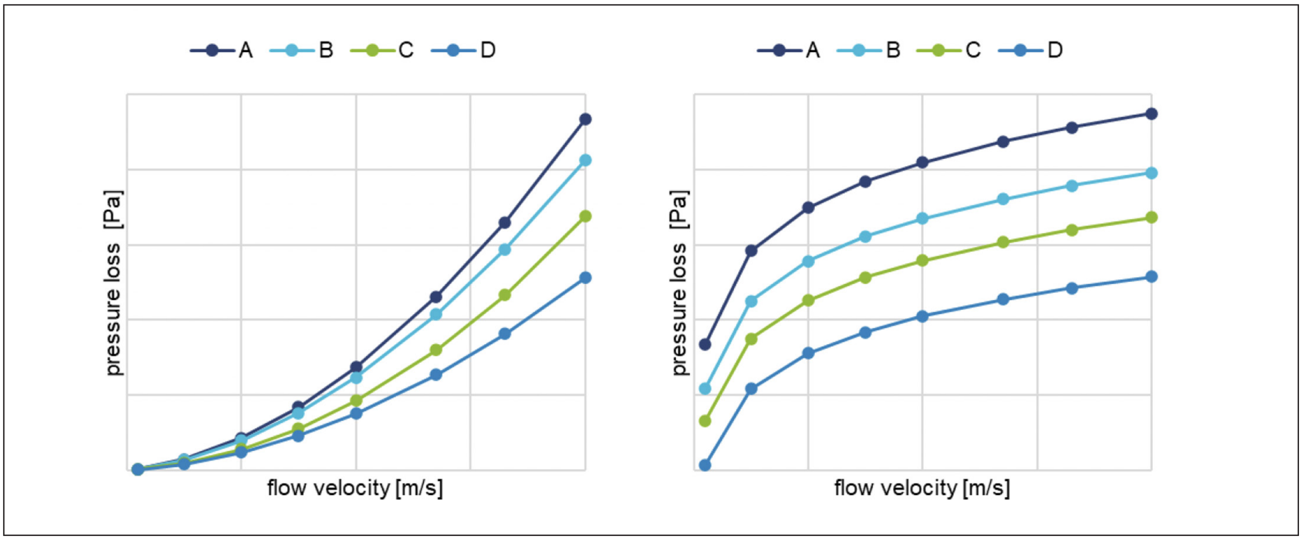

9. Comparison of predicted pressure loss by computation fluid dynamics (CFD) simulation for water (left) and furnish (right).

nian fluids is proportional to the square of the flow velocity. In contrast, the fiber suspension exhibits a different pressure loss behavior that agrees with the theory and experimental results of Duffy and Ventura et al. [17,18]. Based on their research observations, the main reason for this fluidic behavior is the transition from laminar to turbulent flow. At relatively low flow velocities, the flow within the hole is laminar due to a small Reynolds number. As the flow velocity and the Reynolds number increases, the flow becomes turbulent. Under these flow conditions, the pressure loss behavior resembles that of water, with the transition zone defined by the inflection region between the two pressure loss curve types. Another impact factor is the fiber length, which cannot be considered directly in the CFD simulation due to numerical limitations of the used Eulerian single-phase approach. The fiber length can only be considered if it is included in the rheological behavior of the fluid. However, the pressure loss trend for all investigated designs is the same for both water and furnish, making it independent of the fluid type in this context.

The velocity distribution for design A is shown in **Fig. 10** to analyze the general flow physics. For water, a jet is formed due to the strong flow acceleration caused by the drastic reduction in surface area defined by the hole diameter and the open surface of the screen plate. In contrast, for furnish, the small flow velocity results in a considerably smaller shear rate, leading to high local viscosity values and preventing jet formation due to high fluid friction.

The pressure loss for all hole geometries can be analytically determined for water using the extended Bernoulli equation for incompressible flow. This approach considers all specific pressure loss types, such as chamfer acting

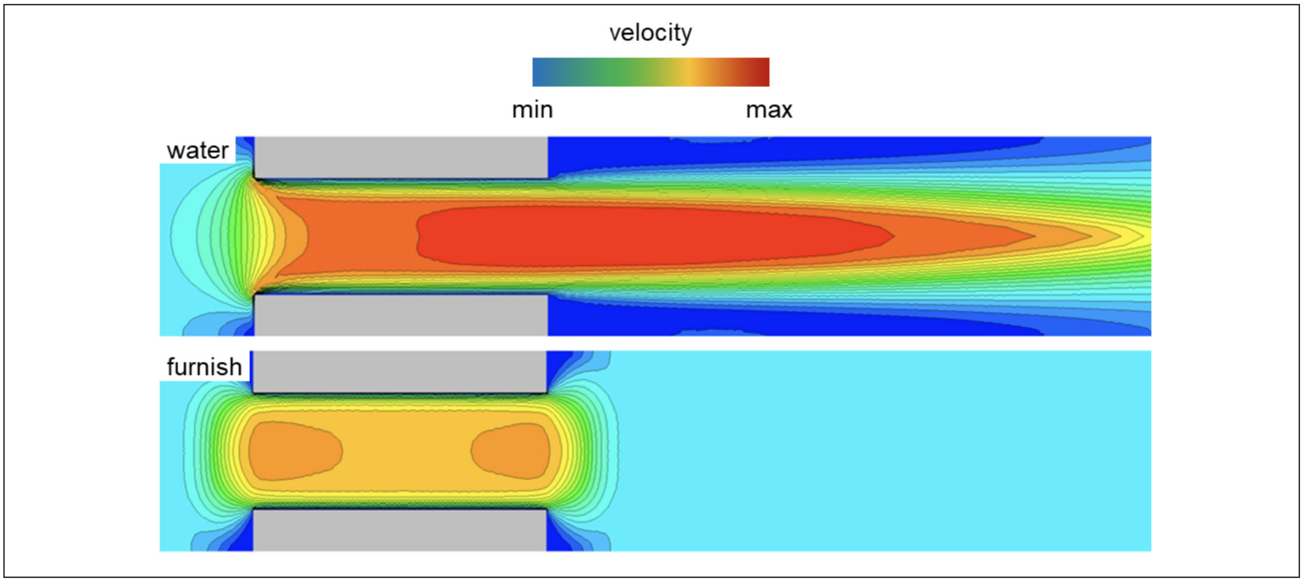

10. Velocity flow field of design A of water (top) and furnish (bottom).

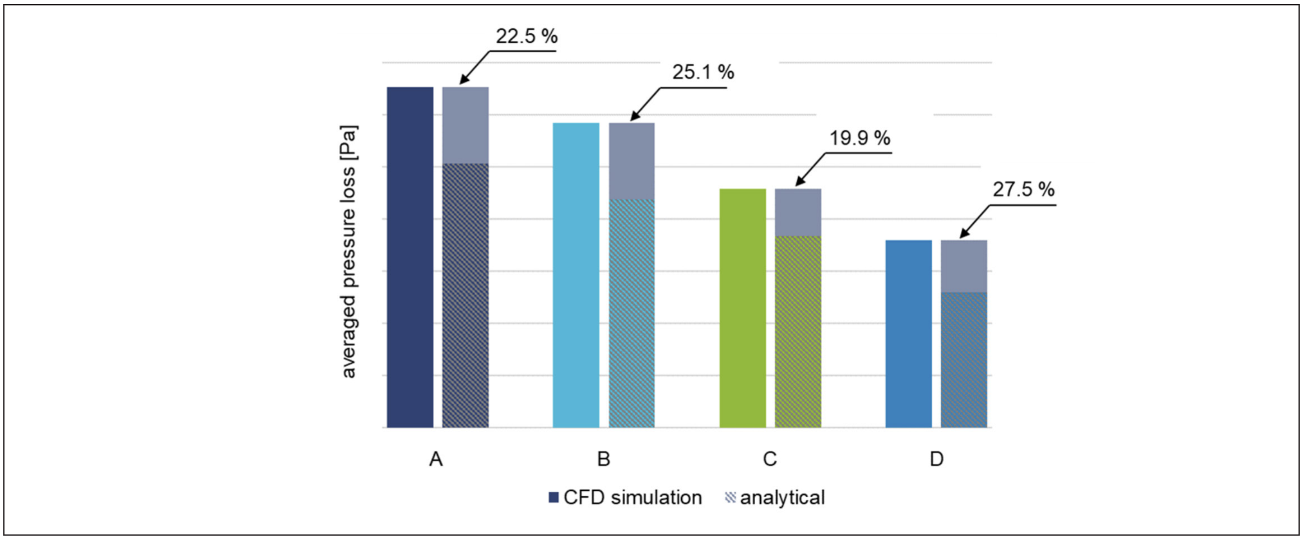

11. Comparison of predicted pressure loss by CFD simulation and analytical model for water.

as continuous nozzle and discontinuous diffuser. The comparison between the numerical results of the CFD simulations with the analytical results are shown in **Fig. 11**. There is only an offset of a few percentage points between the two approaches. Generally, the analytical model underestimates the pressure loss by about 23%. However, the analytical model correctly predicts the pressure loss trend for all four designs and could therefore be used to identify promising hole designs in a short amount of time. For instance, the best hole design could be found analytically by combining the tool with an optimization algorithm using pressure loss as the objective function.

CONCLUSION AND OUTLOOK

In this paper, we demonstrated how knowledge in the field of pulpers can be extended by utilizing CFD simulations as a modern numerical development tool. We carried out two different numerical investigations: one of a pulper equipped with baffles and a rotor (entire device), and another focusing on the screen hole plate design (detailed investigation).

For simplicity, the screen plate was not included in the CFD simulation of the entire pulper. The holes of the screen plate are considerably smaller than the pulper itself, resulting in a large mesh to resolve all occurring flow phenomena. This leads to a high computational effort and potential numerical instabilities. In such a case, a numerical study of different rotor designs would be significantly limited. One approach to solve this problem is to define the screen plate as a porous medium. This is feasible since the flow is redirected within the screen plate such that the flow direction after exiting the screen is predetermined. The porous medium can be implemented within the CFD simulation as a fluid domain where the pressure loss is determined as a function described in this paper. The flow angle and velocity are used as input parameters for the pressure loss function. This approach allows the pressure field of the screen plate to be realized, which could have an additional impact on the rotor flow field and the resulting pulper vortices. This will be investigated numerically in future studies.

In the future, we will focus on the product development supported by state-of-the-art numerical tools like CFD simulations. This can be realized by creating a virtual test rig in which various design ideas can be tested and compared virtually, leading to a reduction of physical trials. This approach can make the development of new products faster and more cost-efficient. **TJ**

ACKNOWLEDGEMENT

The authors would like to thank Mr. Vincent Schäffer for performing the CFD simulations of the screen hole geometries.

LITERATURE CITED

1. Blechschmidt, J., *Taschenbuch der Papiertechnik*, 2nd edn., Hanser Verlag, Munich, 2013.
2. J.M. Voith SE & Co. KG, internal documentation, Heidenheim, 2023.
3. Gorton-Hülgerth, A. and Kerr, J., "Application of Computational Fluid Dynamics in the development and optimization of stock preparation equipment," *PaperCon*, TAPPI Press, Atlanta, 2011.
4. Baldyga, J., Henczky, M., and Makowski, L., *Chem. Eng. Res. Des.* 79(8): 895(2001). https://doi.org/10.1205/02638760152721109.
5. Munz, J. and Schäfer, M., *Case Stud. Chem. Environ. Eng.* 2: 100043(2020). https://doi.org/10.1016/j.cscee.2020.100043.
6. Arratia, P.E., Kukura, J., Lacombe, J., et al., *AIChE J.* 62(7): 2310(2006). https://doi.org/10.1002/aic.10847.
7. Aubin, J., Fletcher, D.F., and Xuereb, C., *Exp. Therm. Fluid Sci.* 28(1): 431(2004). https://doi.org/10.1016/j.expthermflusci.2003.04.001.
8. Aubin, J. and Xuereb, C., *Chem. Eng. Sci.* 61(1): 2913(2006). https://doi.org/10.1016/j.ces.2005.10.075.
9. Blanco, A., Negro, C., Fuente, E., et al., *Chem. Eng. Process.* 46(1): 37(2007). https://doi.org/10.1016/j.cep.2006.04.003.

10. Xie, L., Wang, Q.-A., Luo, X.-J., et al., *Int. J. Chem. Eng.* 17(7): 1(2019). https://doi.org/10.1515/ijcre-2018-0293.

11. Li, Z., Chang, J., Yang, C., et al., *Chem. Eng. Process.* 166(1): 1(2021). https://doi.org/10.1016/j.cep.2021.108463.

12. Britz, M., Grashof, B., and Osti, N., "Numerical simulation of a low consistency single-disc refiner including analysis of experimental rheological data," *TAPPICon*, TAPPI Press, Peachtree Corners, GA, USA, 2021.

13. Ng, K., Fentiman, N.J., Lee, K.C., et al., *Chem. Eng. Res. Des.* 76(6): 737(1998). https://doi.org/10.1205/026387698525315.

14. Menter, F.R., *AIAA J.* 32(8): 1598(1994). https://doi.org/10.2514/3.12149.

15. Hirt, C.W. and Nichols, B.D., *J. Comput. Phys.* 39(1): 201(1981). https://doi.org/10.1016/0021-9991(81)90145-5.

16. Schäffer, V., "Numerische Untersuchung des Strömungseinflusses unterschiedlicher Siebplattenlochgeometrien auf die Effizienz eines exzentrischen Rührbottichs zum Einsatz in der Stoffaufbereitung von Papiermaschinen" (in German), T2000 student research project thesis, DHBW Heidenheim, Germany, 2020.

ABOUT THIS PAPER

Cite this article as:
Britz, M., Grashof, B., Gommel, A., et al., *TAPPI J.* 24(4): 185(2025). https://doi.org/10.32964/TJ24.4.185

DOI: https://doi.org/10.32964/TJ24.4.185

ISSN: 0734-1415

Publisher: TAPPI Press

About this journal

17. Duffy, G.G., *Appita J.* 48(1): 51(1995).

18. Ventura, C., Garcia, F., Ferreira, P., et al., *TAPPI J.* 7(8): 20(2008). https://doi.org/10.32964/TJ7.8.20.

ABOUT THE AUTHORS

We studied this topic because we wanted to get detailed insight into the complex flow system of the pulp-mixing process and its components. Furthermore, we wanted to demonstrate to the paper community how powerful and useful computational fluid dynamics (CFD) simulations are to support, as well as accelerate, the development process.

Previous researchers have only shown that it is possible to simulate a vertical pulper. We went one step further and compared different rotor designs with measurements and looked deep inside the pulper's flow system. To our best knowledge, this marked the first time a numerical study regarding several screen hole plate geometries with different fluid types was performed.

The simulation of free surface flow is quite complex due to the high mesh quality required. We mastered this challenge by an intelligent mesh generation. Furthermore, we introduced a smart periodicity strategy to easily simulate screen plate hole geometries.

Through this study, we learned that it is crucial to compare numerical results with measurements, especially trends, to get a trustworthy numerical model. Only based on such a validated model can virtual product development be performed without any doubts.

It was interesting to find that the numerical results of the rotor power fit very well with the experimental data. Also, the clearly different flow behavior caused by the fluid definition (water vs. furnish) within the screen holes was quite surprising.

Using CFD simulations as presented in this scientific work, the pulping process can be designed more efficiently regarding reduction of both energy consumption and carbon footprint. Our next step is to merge the separately conducted numerical investigations of pulper and screen hole plate by implementing a porous domain with pressure loss information in the pulper model. Additionally, unsteady simulations are planned.

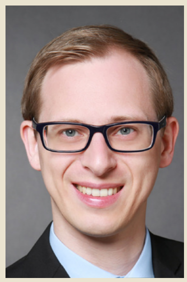

Britz

Grashof

Gommel

Gottschalk

Luedtke

Mueller

Britz is lead expert CFD Simulation, and Grashof is head of Design Calculation for J.M. Voith SE & Co. KG in Heidenheim, Germany. Gommel is head of Pulping, Screening, and Cleaning; Gottschalk is manager, GD&S; Luedtke is global product manager, Dewatering Wear Parts; and Mueller is global product manager, Pulping, for J.M. Voith SE & Co. KG in Ravensburg, Germany. Email Britz at Marcus.Britz@voith.com.